

## KLOE recent results

KLOE collaboration<sup>a</sup>

*presented by V. Patera, INFN, Laboratori Nazionali di Frascati  
via E. Fermi 40, Frascati, Italy*

Since april 1999, the KLOE experiment at DAΦNE has collected about  $200 \text{ pb}^{-1}$  of data, produced in  $e^+e^-$  collision at the c.m. energy of 1020 MeV, the mass of the  $\phi$  meson. These data have been used for detailed studies on the  $\phi$  radiative decays, as well as on rare  $K_S^0$  decays. The first results, based on the  $\sim 20 \text{ pb}^{-1}$  collected in year 2000 are presented here.

### 1 Introduction

The KLOE<sup>1</sup> detector at DAΦNE<sup>2</sup>, the Frascati  $\phi$ -factory, has begun physics data taking in april 1999. The machine operates at the peak of the  $\phi(1020)$  meson production cross section from  $e^+e^-$  collisions with a yield of  $\simeq 3 \times 10^6 \phi$  produced for every delivered  $\text{pb}^{-1}$ . With a peak design luminosity of  $5 \times 10^{32} \text{ cm}^{-2}\text{s}^{-1}$  DAΦNE could deliver as many as  $40 \text{ pb}^{-1}/\text{day}$ , being therefore an exceptional source of almost monochromatic  $K_S^0$  and  $K_L^0$  pairs,  $K^+$  and  $K^-$  pairs, and all other  $\phi$  decay products.

At present DAΦNE reaches a peak luminosity of  $\simeq 5 \times 10^{31} \text{ cm}^{-2}\text{s}^{-1}$  and delivers routinely  $\simeq 2 \text{ pb}^{-1}/\text{day}$ . This is already the highest luminosity ever reached at these energies and is the result of a constant improvement of performances along time. In the present paper the first KLOE results on  $K_S^0$  decays and radiative  $\phi$  decays based on the year 2000 data are presented.

### 2 The KLOE detector

The KLOE detector<sup>1,3</sup> consists of a large tracking chamber, and a hermetic electromagnetic calorimeter. A large magnet, which consists of a superconducting coil and an iron yoke surrounding the whole detector, provides an axial magnetic field of 0.52 T.

---

<sup>a</sup>A. Aloisio, F. Ambrosino, A. Antonelli, M. Antonelli, C. Bacci, G. Bencivenni, S. Bertolucci, C. Bini, C. Bloise, V. Bocci, F. Bossi, P. Branchini, S. A. Bulchjov, R. Caloi, P. Campana, G. Capon, G. Carboni, M. Casarsa, V. Casavola, G. Cataldi, F. Ceradini, F. Cervelli, F. Cevenini, G. Chieffari, P. Ciambone, S. Conetti, E. De Lucia, G. De Robertis, P. De Simone, G. De Zorzi, S. Dell'Agnello, A. Denig, A. Di Domenico, C. Di Donato, S. Di Falco, A. Doria, M. Dreucci, O. Erriquez, A. Farilla, G. Felici, A. Ferrari, M. L. Ferrer, G. Finocchiaro, C. Forti, A. Franceschi, P. Franzini, C. Gatti, P. Gauzzi, S. Giovannella, E. Gorini, F. Grancagnolo, E. Graziani, S. W. Han, M. Incagli, L. Ingrosso, W. Kluge, C. Kuo, V. Kulikov, F. Lacava, G. Lanfranchi, J. Lee-Franzini, D. Leone, F. Lu, M. Martemianov, M. Matsyuk, W. Mei, L. Merola, R. Messi, S. Miscetti, M. Moulson, S. Mueller, F. Murtas, M. Napolitano, A. Nedosekin, F. Nguyen, M. Palutan, L. Paoluzzi, E. Pasqualucci, L. Passalacqua, A. Passeri, V. Patera, E. Petrolo, L. Pontecorvo, M. Primavera, F. Ruggieri, P. Santangelo, E. Santovetti, G. Saracino, R. D. Schamberger, B. Sciascia, A. Sciubba, F. Scuri, I. Sfiligoi, T. Spadaro, E. Spiriti, G. L. Tong, L. Tortora, E. Valente, P. Valente, B. Valeriani, G. Venanzoni, S. Veneziano, A. Ventura, G. Xu, G. W. Yu

The tracking chamber<sup>4</sup> (dc) is a cylindrical, 2 m radius, 3.3 m long drift chamber. The total number of wires is 52140, out of which 12582 are the sense wires. It operates with a low-Z, He gas mixture, to minimize multiple scattering of charged particles and regeneration of  $K_L^0$ . The 58 concentric layers of wires are strung in an all-stereo geometry, with constant inward radial displacement at the chamber center. A spatial resolution better than  $200\mu\text{m}$  is obtained. The momentum resolution for 510 MeV/c electrons and positrons is 1.3 MeV/c, in the angular range  $130^\circ > \theta > 50^\circ$ .

The electromagnetic calorimeter<sup>3,5</sup> (EmC) is a lead-scintillating fibers sampling calorimeter, divided into a barrel section and two endcaps. The modules of both sections are read-out at the two ends by a total of 4880 photomultipliers. In order to minimize dead zones in the overlap region between barrel and endcaps, the modules of the latter are bent outwards with respect to the decay region.

The calorimeter was designed to detect with very high efficiency photons with energy as low as 20 MeV and to accurately measure their energy and time of flight. Calibrations of energy and time scales are performed simultaneously using appropriate data sub-samples during data collection. An energy resolution of  $5.7\%/\sqrt{E(\text{GeV})}$  is achieved throughout the whole calorimeter, together with a linearity in energy response better than 1% above 80 MeV and better than 4% between 20 to 80 MeV.

Moreover,  $\gamma$  samples from different processes are selected to measure the time resolution at various energies; it scales according to the law  $\sigma_t = (54/\sqrt{E(\text{GeV})} \oplus 50)$  ps.

At the present luminosity then KLOE trigger system<sup>6</sup> acquires data at a rate of  $\sim 2.5$  khz, resulting in a throughput to the daq system<sup>7</sup> of  $\sim 3$  mbytes/s. the data are reconstructed quasi-on line by a dedicated computer farm, whose computing power exceeds 5000 specsints<sup>95</sup>.

### 3 $K_S^0$ decays

When a  $\phi$  meson decays into two neutral kaons,  $c$ -invariance forces the two kaons to be in a  $K_S^0$ - $K_L^0$  state. The observation of a  $K_L^0$ , therefore, *tags* the presence of the  $K_S^0$  in the opposite hemisphere. Moreover, at DAΦNE  $K_S^0$  is produced with a 110 MeV/c momentum and its decay occurs very close to the interaction point.

The determination of the ratio of the partial decay widths into two charged and into two neutral pions is presented. This ratio is relevant to the main KLOE physical item, the CP violation in the  $K_L^0$  -  $K_S^0$  system, since it is a part of the double ratio from which the CP violation parameter  $\text{Re}(\epsilon'/\epsilon)$  is derived. Moreover it is of interest for low energy hadron phenomenology, especially if the radiation of soft photons in the charged decay is properly taken into account<sup>9</sup>. We present also the measurement of the branching ratio of the decay  $K_S^0 \rightarrow \pi^\pm e^\mp \nu$ .

These data correspond to a integrated luminosity of  $\sim 17 \text{ pb}^{-1}$ , acquired with the detector in near perfect and stable conditions.

As  $K_S^0$  tagging strategy, one can look for a  $K_L^0$  interaction in the EmC by searching for an EmC cluster of energy deposit compatible with that due to a slowly moving ( $\beta \approx 0.22$ ) neutral particle (called a 'KCRASH' event). Actually, more than one half of the  $K_L^0$ 's reach the calorimeter before they decay. Thus, the 'KCRASH' tag provides a particularly clean, abundant  $K_S^0$  mesons sample.

#### 3.1 $K_S^0 \rightarrow \pi^+\pi^-$ and $K_S^0 \rightarrow \pi^0\pi^0$ decays

The  $K_S^0$  decaying into two neutral pions events are selected by requiring the presence of at least three EmC clusters with a timing compatible with the hypothesis of being due to prompt photons (within  $5 \sigma$ 's), and energy larger than 20 MeV. The efficiency for detecting a photon of given energy/angle has to be properly evaluated: this is done with real data using  $\gamma$ 's in the decays

$\phi \rightarrow \pi^+\pi^-\pi^0$  as a control sample. The final selection efficiency for the  $K_S^0 \rightarrow \pi^0\pi^0$  decay channel is  $\epsilon_{00}=(90.1\pm0.5)\%$ , dominated by acceptance. the selection of  $K_S^0 \rightarrow \pi^+\pi^-$  events proceeds through asking for two oppositely charged tracks with polar angle in the interval  $30^\circ < \theta < 150^\circ$ , originating in a cylinder of 4 cm radius and 10 cm length around the interaction point. A further cut is applied on the measured momenta to remove the residual background due to charged kaon tracks:  $120 < p(\text{MeV}/c) < 300$ .

The track reconstruction efficiency is measured in momentum and polar angle bins from data subsamples. The final selection efficiency is  $\epsilon_{+-}=(58.5\pm0.1)\%$ , again dominated by acceptance.

The trigger efficiency is determined with real data for both decay types. it is  $(99.69 \pm 0.03)\%$  for the neutral decay and  $(96.5 \pm 0.1)\%$  for the charged one. The above figure includes also the probability for having at least one good cluster to determine the  $t_0$  of the event. Background levels are kept well below 1% for both decay types. The final result is <sup>10</sup>

$$\frac{\Gamma(k_s^0 \rightarrow \pi^+\pi^-)}{\Gamma(k_s^0 \rightarrow \pi^0\pi^0)} = 2.239 \pm 0.003_{\text{stat}} \pm 0.015_{\text{syst}} \quad (1)$$

to be compared with the present PDG (particle data group) value  $2.197 \pm 0.026$ . It is noteworthy that our measurement is a fully inclusive measurement of  $K_S^0 \rightarrow \pi^+\pi^-(\gamma)$ , whereas the experiments quoted in the PDG do not have a clear indication of the cut on the photon energy and the corresponding efficiency.

### 3.2 $K_S^0 \rightarrow \pi^\pm e^\mp \nu$ decays

In order to search for  $K_S^0 \rightarrow \pi^\pm e^\mp \nu$  decay candidates, events with a KCRASH and two oppositely charged tracks from the interaction region are initially selected. events are then rejected if the two tracks invariant mass (in the pion hypothesis) and the resulting  $K_S^0$  momentum in the  $\phi$  rest frame are compatible with those expected for a  $K_S^0 \rightarrow \pi^+\pi^-$  decay, which is three orders of magnitude more abundant. According to monte carlo, this preselection has an efficiency, after the tag, of  $\sim 62.4\%$  on the signal.

In order to perform a time of flight identification of the charged particles, both tracks are required to be associated with an EmC cluster. The acceptance for such a request, estimated by monte carlo, is  $(51.1 \pm 0.2)\%$ . The efficiency on the signal, estimated by means of  $K_L^0$ 's decaying into  $\pi e \nu$  before the dc internal wall, is  $(82.0\pm0.7)\%$ .

All efficiencies related to trigger, track to cluster association, good  $t_0$  determination, are measured directly on data, making use of  $K_L^0 \rightarrow \pi^\pm e^\mp \nu$ ,  $\phi \rightarrow \pi^+\pi^-\pi^0$  and  $K_S^0 \rightarrow \pi^+\pi^-$  subsamples. The product of these efficiencies is  $(81.7 \pm 0.5)\%$ .

Once all the particles identities and momenta are known, the event can be kinematically closed. The  $K_S^0$  momentum is estimated making use of the measured direction of the  $K_L^0$  and of the  $\phi$  4-momentum. The missing energy and momentum of the  $K_S^0$  - $\pi$ -e system are then computed. Their difference is distributed as in figure 1; it must be equal zero for the signal. Data are fitted using mc spectra for both signal and background.

The measured yield is  $N(K_S^0 \rightarrow \pi^\pm e^\mp \nu) = 627 \pm 30$  events, for a total efficiency of  $(21.8 \pm 0.3)\%$ . The total number of events is then divided by the number of observed  $K_S^0 \rightarrow \pi^+\pi^-$  events, to give <sup>11</sup>  $\text{BR}(K_S^0 \rightarrow \pi^\pm e^\mp \nu) = (6.92 \pm 0.34_{\text{stat}} \pm 0.15_{\text{syst}}) \times 10^{-4}$ . This result should be compared with  $\text{BR}(K_S^0 \rightarrow \pi^\pm e^\mp \nu) = (6.70 \pm 0.07) \times 10^{-4}$ , obtained using the  $K_S^0$  and  $K_L^0$  lifetimes and  $\Gamma(K_S^0 \rightarrow \pi^\pm e^\mp \nu) = \Gamma(K_L^0 \rightarrow \pi^\pm e^\mp \nu)$  which follows from  $CPT$  invariance and  $\Delta S = \Delta Q$ . A precise measurement of this decay is a test of the  $\Delta S = \Delta Q$  rule.

## 4 Radiative $\phi$ decay : $\text{BR}(\phi \rightarrow \eta' \gamma)$

The branching ratio of the decay  $\phi \rightarrow \eta' \gamma$  is particularly interesting since its value can probe the  $|s\bar{s}\rangle$  and gluonium content of the  $\eta'$ . In particular, the ratio of its value to the one of  $\phi \rightarrow \eta \gamma$

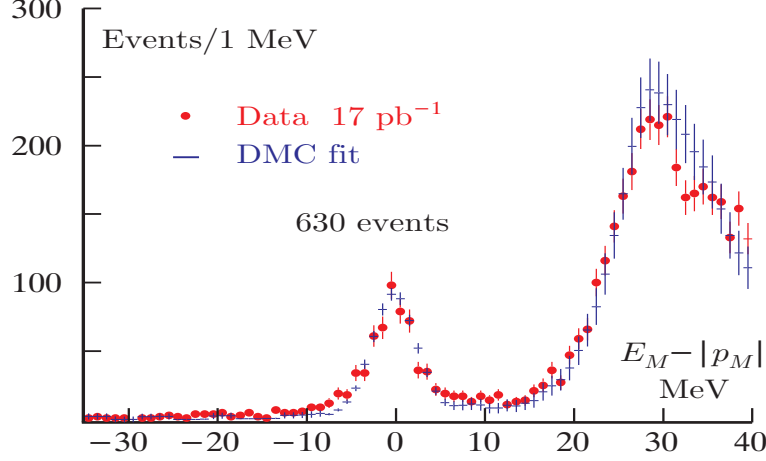


Figure 1: Distribution of the difference between missing energy and missing momentum for  $K_S^0 \rightarrow \pi^\pm e^\mp \nu$  candidates. The peak at zero is the signal. The distribution is fit to the monte carlo of signal and background in the range  $-40 \text{ MeV} + 40 \text{ MeV}$ .

can be related to the  $\eta - \eta'$  mixing parameters, offering an important point of comparison for the chiral perturbation theory.

The decay chain considered in KLOE for the  $\eta'$  selection is  $\phi \rightarrow \eta' \gamma$  with  $\eta' \rightarrow \pi^+ \pi^- \eta$  and then  $\eta \rightarrow \gamma \gamma$ <sup>8</sup>. The  $\eta$  is instead selected in the chain  $\phi \rightarrow \eta \gamma$  with  $\eta \rightarrow \pi^+ \pi^- \pi^0$  and  $\pi^0 \rightarrow \gamma \gamma$ .

In both cases the final state is  $\pi^+ \pi^- \gamma \gamma \gamma$ , resulting in several systematic errors cancellation in the measurement of the ratio  $\text{BR}(\phi \rightarrow \eta' \gamma) / \text{br}(\phi \rightarrow \eta \gamma)$ . For both channels events are selected requiring the presence of three prompt photons and two tracks of opposite charge with a vertex near the interaction region. Then a preliminary kinematic fit is performed requiring total energy and momentum conservation, the constraint  $\beta = 1$  for all photons, without any invariant mass constraint on intermediate particles. Simple kinematic cuts eliminate the background mainly due to  $\phi \rightarrow \pi^+ \pi^- \pi^0$  and to  $\phi \rightarrow K_L K_S \rightarrow \pi^+ \pi^- \pi^0 \pi^0$  events.

The number of signal events is  $N_{ev} = 124 \pm 12_{stat} \pm 5_{syst}$ . The ratio  $\text{BR}(\phi \rightarrow \eta' \gamma) / \text{BR}(\phi \rightarrow \eta \gamma)$  is obtained by normalizing to the number of  $\phi \rightarrow \eta \gamma$  observed events and correcting for detection efficiency taken from MC. The KLOE preliminary result is then<sup>8</sup>:

$$\frac{\text{BR}(\phi \rightarrow \eta' \gamma)}{\text{BR}(\phi \rightarrow \eta \gamma)} = (5.3 \pm 0.5_{stat} \pm 0.4_{syst}) \times 10^{-3} \quad (2)$$

Making use of  $\text{BR}(\phi \rightarrow \eta \gamma)$  value from PDG, a preliminary KLOE value is obtained<sup>8</sup>:

$$\text{BR}(\phi \rightarrow \eta' \gamma) = (6.8 \pm 0.6_{stat} \pm 0.5_{syst}) \times 10^{-5} \quad (3)$$

## 5 Radiative $\phi$ decay : $\text{BR}(\phi \rightarrow f_0 \gamma \rightarrow \pi^0 \pi^0 \gamma)$ and $\text{BR}(\phi \rightarrow a_0 \gamma \rightarrow \eta \pi^0 \gamma)$

The several models proposed to explain the nature of the  $f_0$  and  $a_0$  mesons (ordinary qq meson, qqqq state, KK molecule) make different predictions<sup>12,13</sup> of  $\text{BR}(\phi \rightarrow f_0 \gamma)$ ,  $\text{BR}(\phi \rightarrow a_0 \gamma)$  and their ratio. Therefore a precise measurement of  $\text{BR}(\phi \rightarrow f_0 \gamma) / \text{BR}(\phi \rightarrow a_0 \gamma)$  ratio would clarify the interpretation on the nature of these mesons. The  $f_0$  meson at KLOE has been studied in the following decay chains :  $\phi \rightarrow f_0 \gamma$  with  $f_0 \rightarrow \pi^0 \pi^0$ . The  $a_0$  has been investigated in the channel:  $\phi \rightarrow a_0 \gamma$  with the  $a_0 \rightarrow \eta \pi^0$  and the following decays of the  $\eta$ :  $\eta \rightarrow \gamma \gamma$  and  $\eta \rightarrow \pi^+ \pi^- \pi^0$ . all these final states have 5  $\gamma$ 's.

With the exception of the very clean case of the  $a_0$  production where the final state is  $\pi^+ \pi^- 5\gamma$ , the main backgrounds come from the resonant process  $\phi \rightarrow \rho^0 \pi^0$  with  $\rho^0 \rightarrow \pi^0 \gamma$  or  $\rho^0 \rightarrow \eta \gamma$ , and the continuum process  $e^+ e^- \rightarrow \omega \pi^0$  with  $\omega \rightarrow \pi^0 \gamma$  or  $\omega \rightarrow \eta \gamma$ .

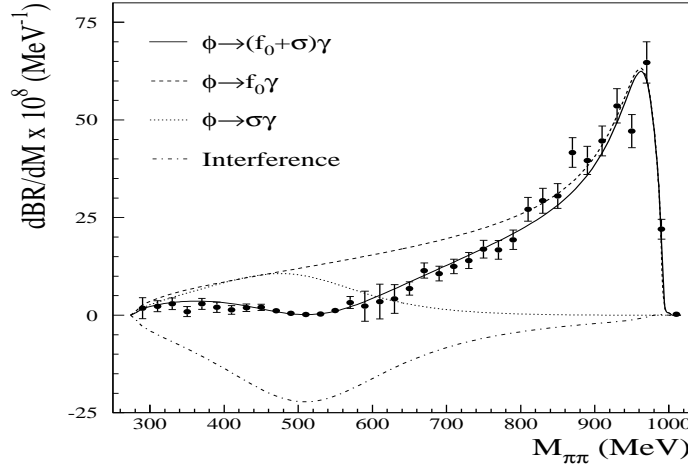


Figure 2:  $dBR/dM$  as a function of  $M_{\pi\pi}$  from  $\phi \rightarrow f_0\gamma$  and  $f_0 \rightarrow \pi^0\pi^0$ . Points are data. The solid line is the fit resulting from assuming a  $f_0$ , a  $\sigma$  and the interference between them. contributions of individual terms are also shown.

The events are identified by requiring five prompt photons within loose acceptance cuts. Then kinematic fits are performed requiring total energy and momentum conservation with the additional constraint  $\beta = 1$  for all photons. Background events are isolated by means of cuts on kinematic variables and on the  $\chi^2$  probability values obtained in the kinematic fits.

The overall detection efficiency is obtained by tuning the MC to reproduce the observed  $M_{\pi^0\pi^0}$  and  $M_{\eta\pi^0}$  invariant mass distributions in case of  $\phi \rightarrow \pi^0\pi^0\gamma$  and  $\phi \rightarrow \eta\pi^0\gamma$  events, respectively.

In the  $\phi \rightarrow \pi^0\pi^0\gamma$  mode the  $M_{\pi^0\pi^0}$  spectrum can have contribution by the process  $\phi \rightarrow S\gamma$ , with the scalar meson  $S \rightarrow \pi^0\pi^0$ , and by  $\phi \rightarrow \rho^0\pi^0$ , with  $\rho^0 \rightarrow \pi^0\gamma$ <sup>12</sup>. We considered the contribution of the  $f_0$  and  $\sigma$ <sup>14</sup> scalar mesons to fit the dipion spectrum, as shown in fig 2. Is clearly visible the negative interference with the  $\sigma$  term, while is negligible the contribution from the  $\phi \rightarrow \rho^0\pi^0$  channel. The following results are obtained integrating the  $f_0$  component of the spectrum<sup>12</sup>:

$$BR(\phi \rightarrow f_0\gamma \rightarrow \pi^0\pi^0\gamma) = (1.49 \pm 0.07) \times 10^{-4} \quad (4)$$

In the  $\phi \rightarrow \eta\pi^0\gamma$  case the two  $m_{\eta\pi^0}$  spectra obtained for the samples where  $\eta \rightarrow \gamma\gamma$  and  $\eta \rightarrow \pi^+\pi^-\pi^0$  (fig 3) are fit together setting the  $a_0$  mass parameter = 984.8 MeV from PDG. From this fit we obtain<sup>13</sup>:

$$BR(\phi \rightarrow a_0\gamma, a_0 \rightarrow \eta\pi^0) = (7.4 \pm 0.7) \times 10^{-5} \quad (5)$$

The presented results on the  $f_0$  and  $a_0$  scalars can be put together to give a ratio<sup>13</sup>:

$$\frac{BR(\phi \rightarrow f_0\gamma)}{BR(\phi \rightarrow a_0\gamma)} = 6.1 \pm 0.6 \quad (6)$$

## 6 Conclusions

The KLOE detector at DAΦNE has collected about 200 pb<sup>-1</sup> of data so far. In this report studies on  $\phi$  radiative decays have been presented, together with precision measurements on two  $K_S^0$  decay channels, based on the statistics accumulated in year 2000. Charged kaon decays as

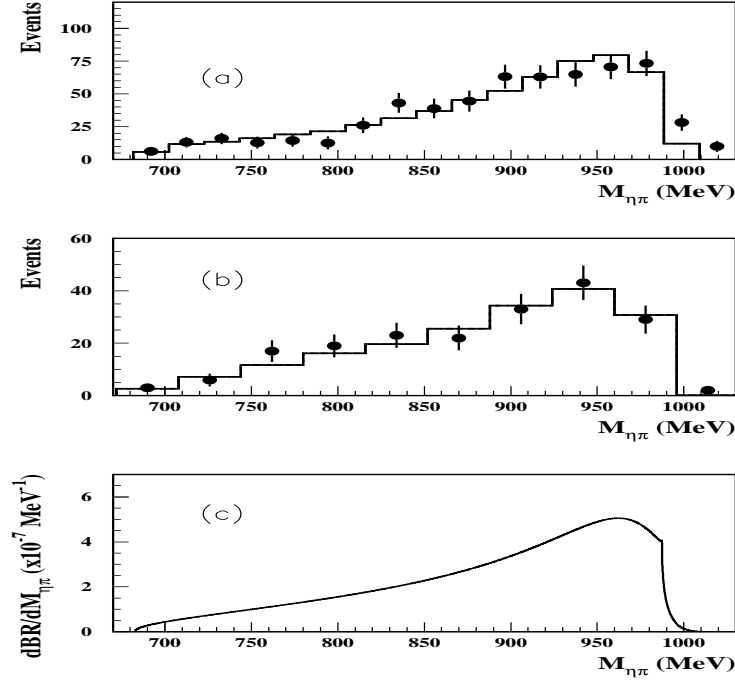


Figure 3: The background subtracted  $M_{\eta\pi}$  spectra resulting from  $\phi \rightarrow a_0\gamma$  and  $a_0 \rightarrow \eta\pi$ . Top plot points are data, for the case where  $\eta \rightarrow 2\gamma$ , middle plot for case where  $\eta \rightarrow \pi^+\pi^-\pi^0$ . Histograms are results of the fit and the theoretical curve for the  $a_0$ .

well as other  $K_S^0$  decays, such as  $K_S^0 \rightarrow 3\pi^0$  or  $K_S^0 \rightarrow \gamma\gamma$  are under investigation. Results on these last topics are expected in a short time.

## Bibliography

1. The KLOE Collaboration, A general purpose detector for DAΦNE , LNF-92/019 (1992).
2. S.Guiducci et al., Proc. of the 2001 Particle Accelerator Conference (Chicago,Illinois,USA), P.Lucas S.Weber ed., 353, (2001)
3. The KLOE Collaboration, The KLOE detector, Technical Proposal, LNF-93/002 (1993).
4. The KLOE Collaboration, The Tracking detector of the KLOE experiment, LNF-01/016 (P) (2001), Submitted to Nucl. Inst. Meth. A.
5. The KLOE Collaboration, The KLOE electromagnetic calorimeter, *Nucl. Inst. Meth. A* **482** 363 (2002)
6. The KLOE Collaboration, The KLOE Trigger System, LNF-02/02 (P) (2002), Submitted to Nucl. Inst. Meth. A.
7. The KLOE Collaboration, The KLOE Data Acquisition System, LNF-95/014 (1995).
8. F. Ambrosino: KLOE Note 179
9. V. Cirigliano, J.F. Donoghue, E. Golowich, *EPJ C* **18**, 83, (2000). B **444** 38, (1998).
10. The KLOE collaboration, hep-ex/0204024, submitted to Phys. Lett. B
11. The KLOE collaboration, *Phys. Lett. B* **535** 37,(2002)
12. The KLOE collaboration, hep-ex/0204013, submitted to Phys. Lett. B
13. The KLOE collaboration, hep-ex/0204012, submitted to Phys. Lett. B
14. E.M.Aitala et al., *Phys. Rev. Lett* **86** 770 (2001)